DETERMINATION OF CRITICAL FLAW SIZE IN GUN LAUNCH 40-mm GRENADE

N. Payne
J. Jablonksi
J. Cordes

December 2010

U.S. ARMY ARMAMENT RESEARCH, DEVELOPMENT AND ENGINEERING CENTER

Munitions Engineering Technology Center

Picatinny Arsenal, New Jersey

20110110644

REPORT DOCUMENTATION PAGE		Form Approved OMB No. 0704-01-0188

The public reporting burden for this collection of information is estimated to average 1 hour per response, including the time for reviewing instructions, searching existing data sources, gathering and maintaining the data needed, and completing and reviewing the collection of information. Send comments regarding this burden estimate or any other aspect of this collection of information, including suggestions for reducing the burden to Department of Defense, Washington Headquarters Services Directorate for Information Operations and Reports (0704-0188), 1215 Jefferson Davis Highway, Suite 1204, Arlington, VA 22202-4302. Respondents should be aware that notwithstanding any other provision of law, no person shall be subject to any penalty for failing to comply with a collection of information if it does not display a currently valid OMB control number.
PLEASE DO NOT RETURN YOUR FORM TO THE ABOVE ADDRESS.

1. REPORT DATE (DD-MM-YYYY) December 2010	2. REPORT TYPE Interim	3. DATES COVERED (From - To) November 2009 to March 2010
4. TITLE AND SUBTITLE DETERMINATION OF CRITICAL FLAW SIZE IN GUN LAUNCHED 40-mm GRENADE		5a. CONTRACT NUMBER
		5b. GRANT NUMBER
		5c. PROGRAM ELEMENT NUMBER
6. AUTHORS N. Payne, J. Jablonksi, and J. Cordes		5d. PROJECT NUMBER
		5e. TASK NUMBER
		5f. WORK UNIT NUMBER
7. PERFORMING ORGANIZATION NAME(S) AND ADDRESS(ES) U.S. Army ARDEC, METC Fuze and Precision Armament Technology Directorate (RDAR-MEF-E) Picatinny Arsenal, NJ 07806-5000		8. PERFORMING ORGANIZATION REPORT NUMBER
9. SPONSORING/MONITORING AGENCY NAME(S) AND ADDRESS(ES) U.S. Army ARDEC, ESIC Knowledge & Process Management (RDAR-EIK) Picatinny Arsenal, NJ 07806-5000		10. SPONSOR/MONITOR'S ACRONYM(S)
		11. SPONSOR/MONITOR'S REPORT NUMBER(S) Technical Report ARMET-TR-10024

12. DISTRIBUTION/AVAILABILITY STATEMENT

Approved for public release; distribution is unlimited.

13. SUPPLEMENTARY NOTES

14. ABSTRACT

The inspection and screening of flaws in high explosive filled gun fire projectiles are crucial to ensure safety for soldiers using these items. In-bore failure of structural components are sure to produce lethal consequences; therefore, it is of great importance to determine what the maximum permissible crack size is for a given component coming off the production floor. The analytical process to determine critical flaw size occurs in two stages. First, ABAQUS Explicit finite element analysis code is used to conduct interior ballistic simulation of a 40-mm shape charge projectile. The modeling scope includes interior gun tube geometry with drive band engraving and spin up effects. Pressure load inputs, which were derived from live-fire test data, are used to drive the model. Secondly, the explicit model results are passed to NASGRO software for critical flaw size determination using linear-elastic fracture mechanics theory. The modeling information and approach to the problem will be presented in this paper as well as explicit model results and proposed inspection criteria.

15. SUBJECT TERMS

Critical flaw size	Engraving	Interior ballistics	Fracture mechanics	Gun launch

16. SECURITY CLASSIFICATION OF:			17. LIMITATION OF ABSTRACT	18. NUMBER OF PAGES	19a. NAME OF RESPONSIBLE PERSON N. Payne
a. REPORT U	b. ABSTRACT U	c. THIS PAGE U	SAR	27	19b. TELEPHONE NUMBER (Include area code) (973) 724-3062

Standard Form 298 (Rev. 8/98)
Prescribed by ANSI Std. Z39.18

CONTENTS

FIGURES

FIGURES
(continued)

INTRODUCTION

The M433 projectile is a 40-mm, low velocity, shaped charge grenade. The grenade carries a fuze device, which upon impact, initiates a billet of high explosive material that then turns a metal liner into a high speed jet of material that penetrates armor plating. During the launching of the grenade, the body is under intense inertial forces that put significant amounts of stress in the material. Any voids or cracks under this type of loading can propagate and cause a breakup of the grenade in-bore. Because this device is used in a hand-held gun system, defective structural parts pose an inherent risk to the soldier and cannot be tolerated. The central objective of the analysis detailed in this report is to determine safe inspection criteria for the structural components of the M433.

Finite element analysis (FEA) methods are used extensively during the design process of a gun fired projectile to ensure the structural integrity and safety of the design. However, these analyses presuppose that the parts are defect free and uniform in characteristic. Since these items are also intended to be produced at a mass scale, a variety of manufacturing methods are relied upon to achieve cost reduction. Often, there is a link between part cost and part quality, with cheaper manufacturing methods being more prone to causing defects in the finished component and thus compromising safety. It is at this point critical flaw size analysis can be used to determine acceptable inspection parameters at the end of the production line. Critical flaw size analysis gives an approximation of the largest permissible crack size that can be tolerated for a given part given stress magnitude and distribution determined in the previous finite element model.

MODELING AND SIMULATION

Modeling Approach

The determination of critical flaw size for a given component requires two separate analysis activities. First, an explicit FEA simulation determines the magnitude and distribution of the peak tensile stresses during the projectile's launch. In the ABAQUS/Viewer postprocessor, the regions that exhibit high stresses are examined and stress distributions, as a function of depth, are generated in tabular form from the output. These stress distributions are then passed to an outside piece of software (NASGRO) using fracture mechanics equations to determine the smallest crack size that will fail the material for the given stress state.

Model Geometry

The M433 projectile geometry is shown in figure 1. A half section view is shown in figure 2. The geometry used in this analysis includes all of the main structural components of the projectile, none of which have been de-featured. The fuze mechanisms have been omitted in the model in order to save computation time. The absent mass was accounted for by increasing the density of the housing material, thus maintaining the appropriate inertia loading on the grenade body.
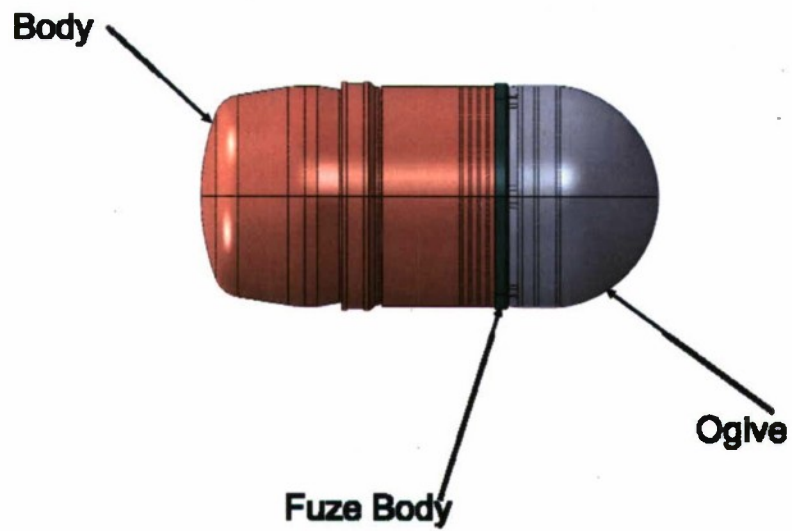
Figure 1
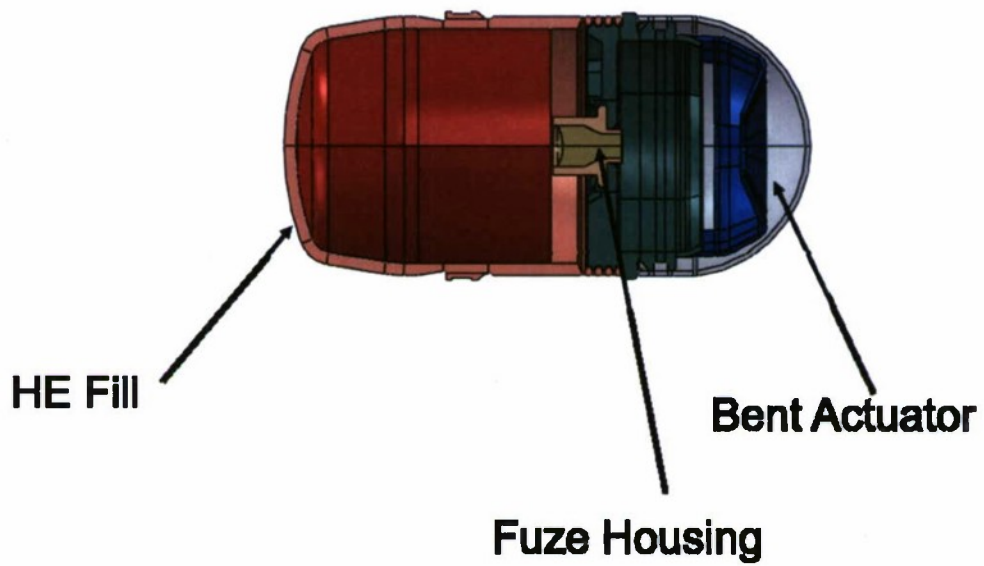M433 projectile assembly

Figure 2
Section view of M433 assembly

The only significant simplification made to a structural component in the model was to the threaded joint between the body and the fuze (fig. 3). The threaded joint, normally a helical thread, was modeled as annular grooves. This enabled the parts to be meshed in a reasonable manner; helping to minimize an already dense mesh in that region. The annular grooves support axial transmission of the loads through the two parts, but do not transmit rotations to allow for torsion between the parts a coupled reference point scheme was used to transmit rotation. Details of this coupling are described later in the Boundary Condition, Loads, and Constraints section.
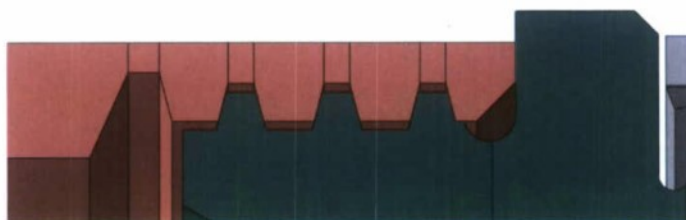

Figure 3
Threaded joint modeled as annular grooves

Material Properties and Assignments (table 1)

Table 1
Material properties

Part	Material	Modulus (psi)	Poisson ratio	Density (lbf*s^2/in.^4)	Yield (psi)	Ultimate true plastic strain (%)	Ultimate true stress (psi)
Drive band	Copper (JC model)	10.1E	0.33	0.000253	**	**	**
Body	Steel type 1009	29E6	0.29	0.00073504	61,407	7.5	71,670
Fuze body	AL 6061 T6 rod	10.1E6	0.33	0.000471*	34,114	9	46,200
Ogive	AL 6061 T6 sheet	10.1E6	0.33	0.00025364	65,121	9	46,200
Comp A5	Comp A5	2.6E6	0.22	0.0001611	NA	NA	NA
Fuze housing w/fill	AL 2017 T4 rod	10.4E6	0.33	0.0002614	32,098	10.74	61,600
Bent actuator	AL 2024 T4 sheet	10.7E6	0.33	0.00025882	40,150	10.68	69,440

*Density increased to account for mass of omitted fuze components.
**Johnson-Cook model parameters were used and are not available for open dissemination.

Boundary Conditions, Loads, and Constraints

To reduce computation and model complexity, the gun tube (shown in white in figure 4) was given a rigid body constraint using reference point no. 4 as the control point. The gun tube was held fixed in all translational and rotational directions using an encastre boundary condition on the tube's rigid body reference node (RP-4). The rigid tube provided the boundary on which the projectile could ride while traveling down the gun tube. Raised interior portions, termed lands, are shown in figure 5 with a helical shape. These lands cut against the drive band on the body and provide the spin up conditions during the analysis.
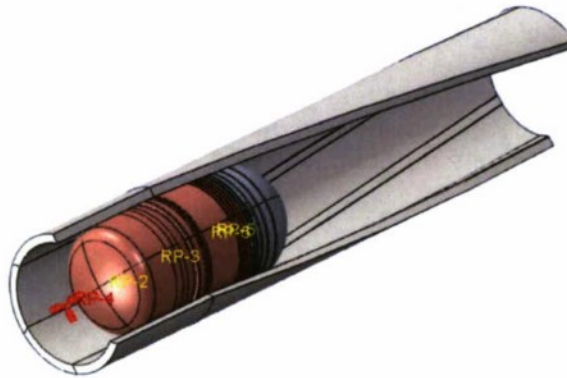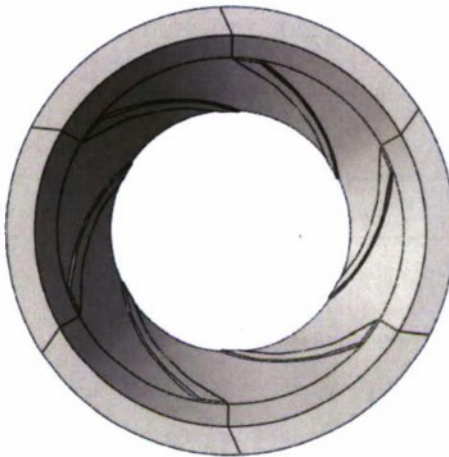
Figure 4
Gun tube assembly with cells removed

Figure 5
Interior of gun tube with rifling

Several tie constraints were used in the model to provide couple motion between parts where adhesives or friction would have been acting in reality. Although it is possible to implement friction in ABAQUS, tie constraints allowed for model simplification and were warranted as the areas in question were not of particular interest. These tie constraints are displayed in figure 6.
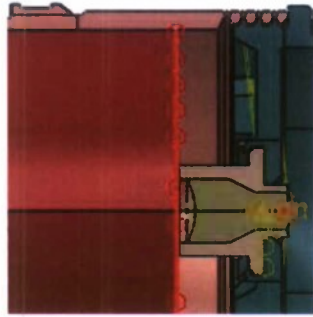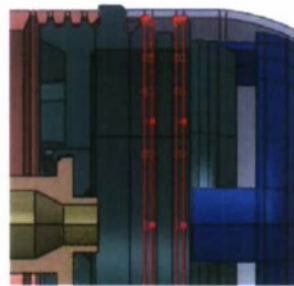
Comp A billet - liner (not shown)

Fuze body - housing

Fuze fill - housing

Fuze body - ogive

Figure 6
Tie constraint

The coupling transmission of spin between the annular grooved surfaces was accomplished using distributed coupling constraints from the grooved surfaces to individual reference points (RP). The surfaces being controlled on each part are shown in figures 7 and 8. The two RPs rotational degrees-of-freedom are then joined using an align connector shown in figure 9. The distribution coupling enforces the motion of the contained nodes in a force based, average way. This method allows for both the contact forces between the parts and other motion constraints imposed on the reference points to influence the parts motion.
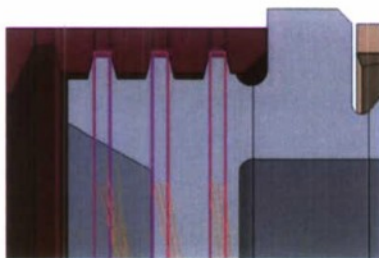

Figure 7
Surfaces on the body coupled to RP
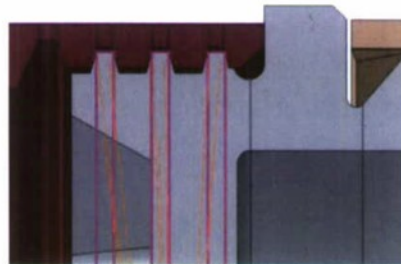
Figure 8
Surfaces on fuze coupled to RP
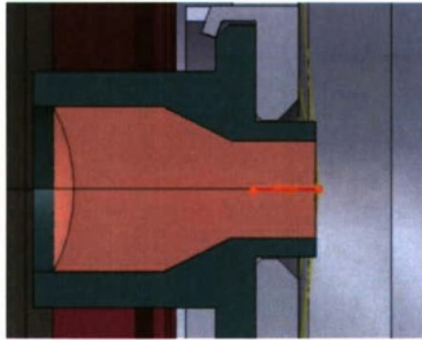
Figure 9
Alignment connector

If perfect obturation (the sealing of propellant gasses behind the projectile) is assumed, the surfaces that receive the applied pressure load are shown in red in figure 10. The pressure-time curve (fig. 11) used to drive this load in the model was derived from instrumented live-fire testing, in which a pressure transducer is tapped into the side of the cartridge case and reads the pressure throughout the duration of the launch.
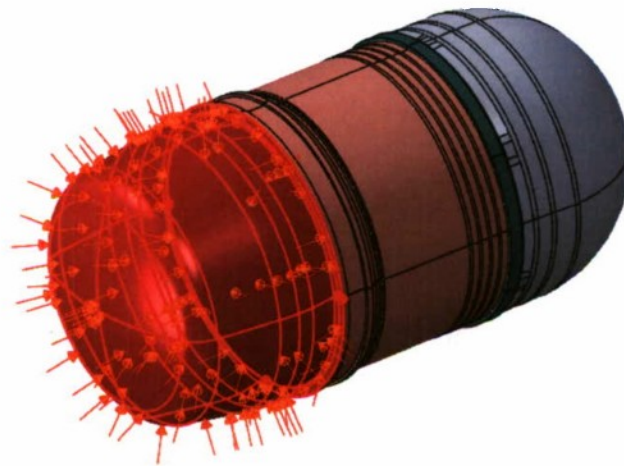
Figure 10
Pressure load applied on base of projectile
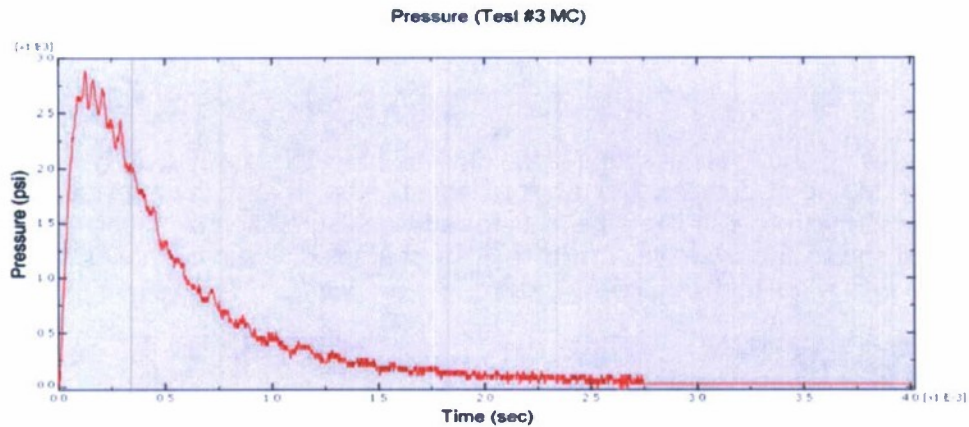
Figure 11
Mid-case pressure data

Mesh Details

The mesh generated for the analysis was significantly denser in quality than is typically used for structural analysis of launched projectiles (figs. 12 and 13). A minimum of six elements were used throughout the thickness of all structural parts (body, fuze, and ogive). This ensures bending stress and the distribution can be accurately resolved through the thickness of the part and is required to yield the appropriate out for critical crack analysis (more on this in Critical Crack Size Determination section).

Figure 12
Detail of sidewall of projectile body

Deformable elements	Nodes
852,480	1,063,527

Figure 13
Meshed assembly

7

SIMULATION RESULTS

Engraving

The engraving and final net shape of the drive band matched very closely with live-fire results. Figures 14 and 15 compare the two resultant shapes. The width of the lead groove corresponds cl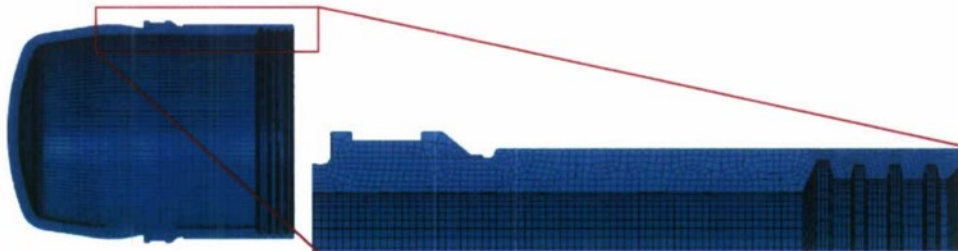osely with one another; the test projectile measured approximately 0.179 in. and the model result shows approximately 0.175 in. Also, characteristics in both results were that the lead groove was wider than the trailing groove.

Figure 14
Engrave mark on recovered projectile
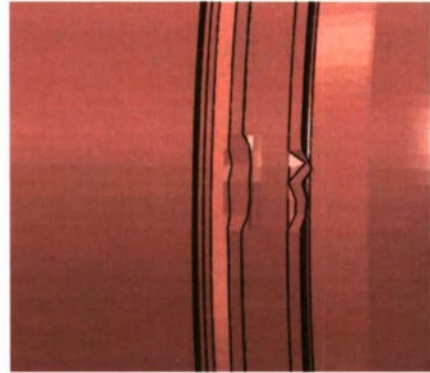
Figure 15
Engrave mark on FEA projectile

During the progression of the engraving (fig. 16), it was also observed that high stresses were localized at the areas of the shearing, which of course is to be expected. However, this stress penetrated through the thickness of the body and formed significant "hot spots" on the inside of the body (fig. 17). These regions alternated from tension to compression and are of particular concern because of the fact that tension enables crack propagation and they are in close proximity to high explosive fill.

Figure 16
Engraving progression

Figure 17
Hoop stress distribution

Stress and Plasticity in Components

The results did not show any amounts of plastic yielding in structural components or material damage that constituted a failure condition or a safety issue for the soldier. Shown in figure 18, there was a very small amount of localized plasticity on the inside of the body corresponding to the engraving hot spots. These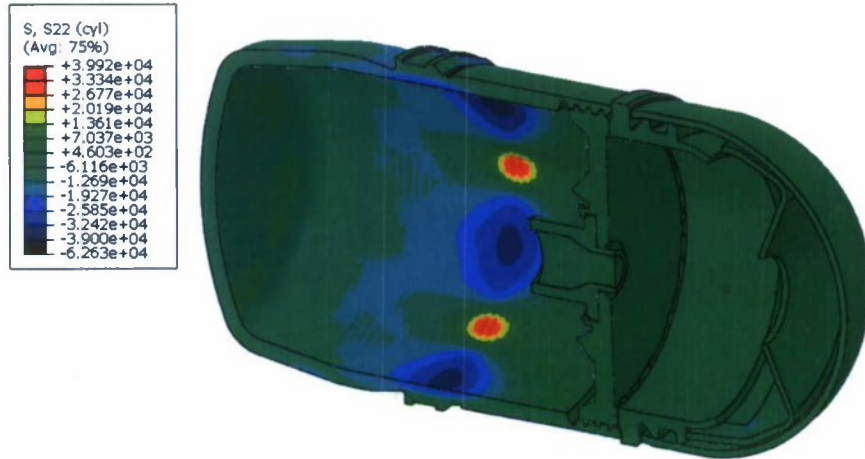 areas of yielding were very small and the peak magnitude was about 0.25%. Conventionally, the maximum allowable yield through a sidewall must be less than one-fourth of the overall sidewall thickness. The plastic resulting yield in the model was much less than this measure. Much more significant plastic yielding occurred in the bent actuator, which was housed within the ogive (fig. 19). Since part is not an integral structural component and is enclosed in the projectile, the plasticity observed in the model is not of concern for the purposes of screening for safety critical failures.
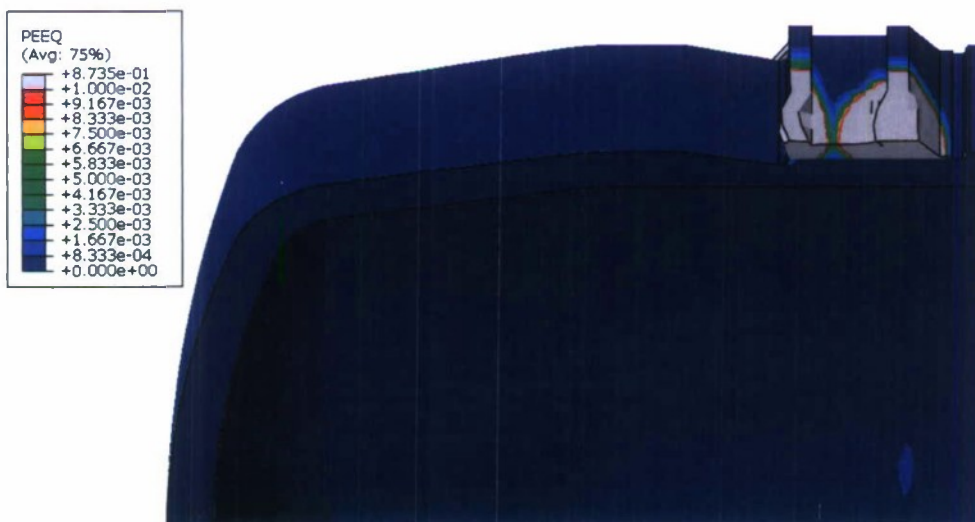
Figure 18
Plastic strain and drive band

9
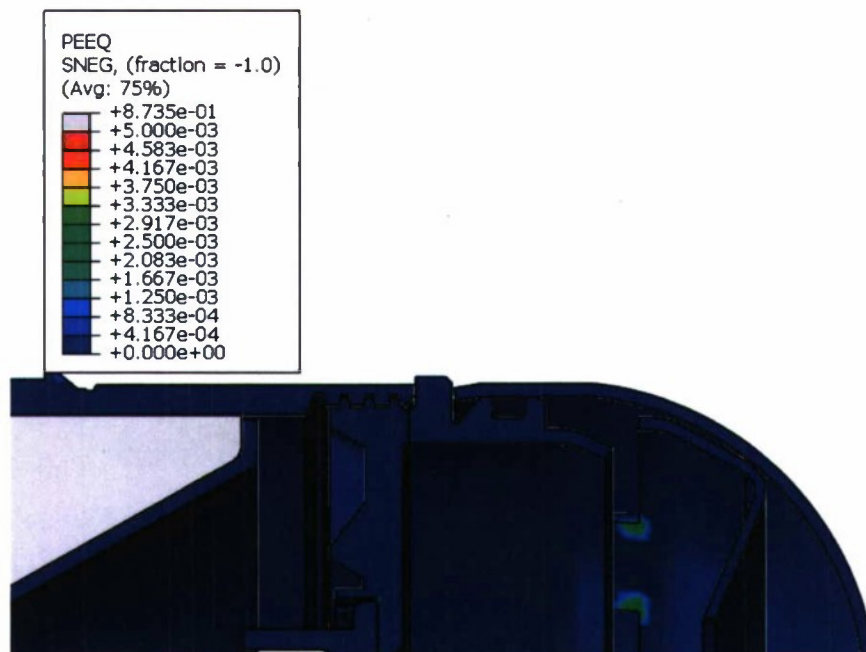
Figure 19
Equivalent plastic strain in the actuator

Model Validation

A quick comparison of the final exit velocity in the model with muzzle velocities measured from live-test firing provides a degree of validation. Shown in figure 20, the exit velocity of the projectile was approximately 247 ft/s. An average muzzle velocity of 120 test shots came to 252 ft/s, a difference of roughly 1.9%.

Figure 20
Plot of axial velocity of projectile

10

CRITICAL CRACK SIZE DETERMINATION

Introduction to Fracture Mechanics

When a crack is present in a structure, it serves to concentrate local stress fields around its tip. As a result, the yield strength of the material can be exceeded around the crack, which may lead to crack propagation. If this propagation becomes self-sustaining or "unstable," the structure will fail due to fracture. Such failure generally occurs due to applied stress perpendicular to the c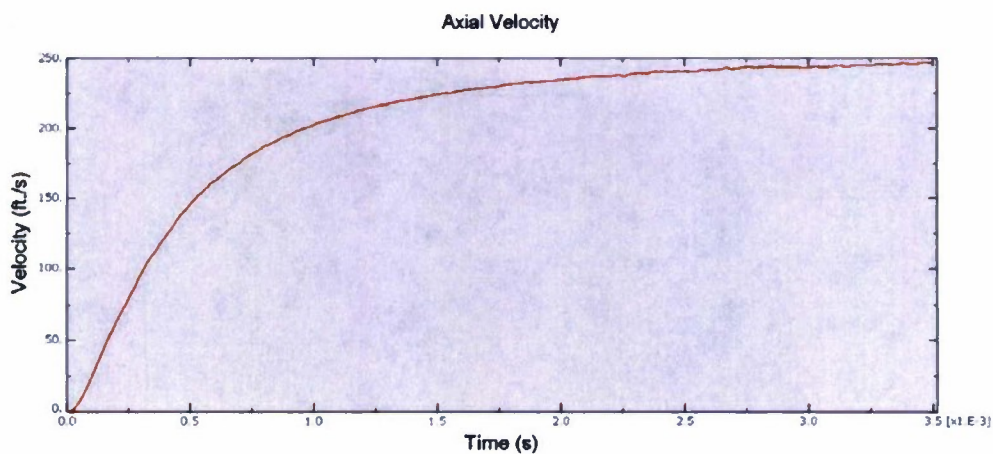rack plane (Mode I), but other modes of failure such as in-plane shear (Mode II) and out-of-plane shear (Mode III) are possible. For example, composite materials with weak fiber-matrix interfaces are prone to Mode II fracture.

Linear elastic fracture mechanics (LEFM) theory establishes the concept of a stress intensity factor that can be used in engineering calculation to predict fracture failure. Stress intensity factors are dependent on several considerations including specimen geometry, loading conditions, and flaw geometry, which makes them very complex to evaluate. However, many closed form solutions for simple cases have been developed. For a given state, if the stress intensity factor exceeds the fracture toughness (a property) of the material, then unstable crack growth will occur causing the structure to fracture.

The LEFM is valid as long as the material under consideration obeys Hooke's Law. In reality, there is often a plastic region formed ahead of a crack tip, which violates these assumptions of LEFM. However, if the plastic region ahead of the crack tip is sufficiently small, the material can be treated as linear elastic.

If a specific specimen geometry, load case, and flaw shape is assumed, it is possible to calculate the crack length required for the stress intensity factor to exceed the fracture toughness of the material. This represents the largest flaw a structure can accommodate before it fails in fracture and is commonly known as the critical crack size.

NASGRO is a computer code that is capable of calculating stress intensity factor. As a result, the software can determine the critical crack size of a defined problem by solving the following equation

$$K_{Ic} - K_I = 0$$

Where K_{Ic} represents the fracture toughness of a material and K_I represents the stress intensity factor. It is important to note that NASGRO only considers Mode I loading. Due to the complex dependence of K_I on multiple variables, the code uses numerical approximation techniques to solve for the roots of the previous equation. With an initial guess of critical crack length, NASGRO implements Newton's method to converge to a solution. In this way, it is possible to determine critical crack sizes.

NASGRO Procedure

NASGRO contains a database of closed-form solutions for stress intensity factors given various specimen geometries, loading cases, and flaw geometries. The user must select an appropriate model for the application being analyzed. Since the current analysis is concerned with determining critical crack sizes caused by manufacturing defects, a pair of surface crack models is selected for use; these are the longitudinal and circumferential surface crack for a hollow cylinder as they most closely resemble the actual shape of the projectile body (known in the code as SC04 and SC05). A schematic of these models is shown in figure 21.
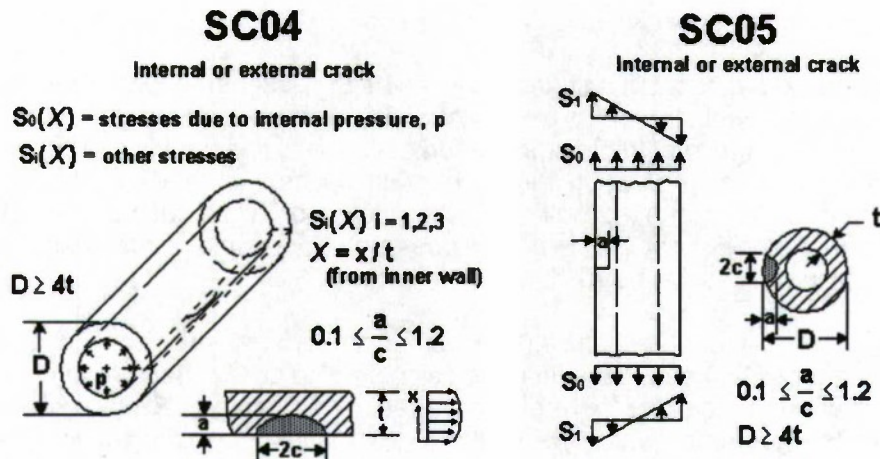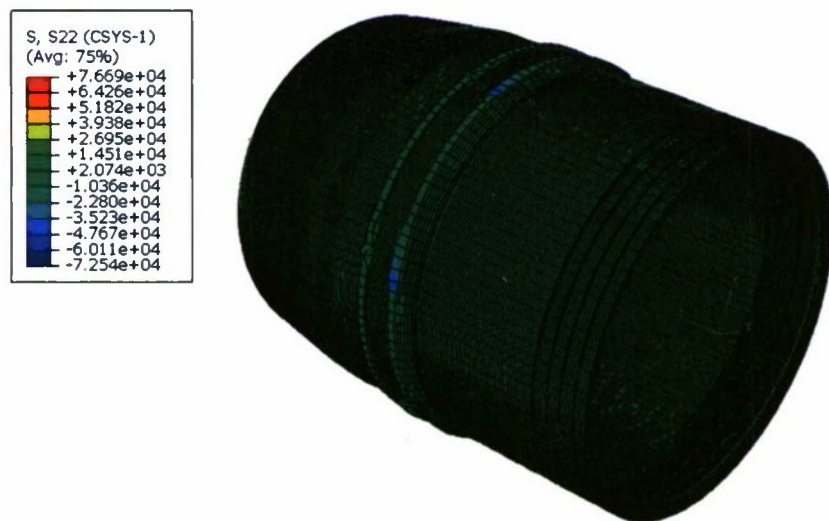
Figure 21
Surface crack models used in NASGRO

Next, the field output from the ABAQUS structural results is transformed from the global default system (fig. 22), to a cylindrical coordinate system. This enables the display of the circumferential (hoop), axial, and radial stress in the sidewall of the grenade body. Since surface cracks are only afforded the possibility of propagating while in a state of tension, the areas of concern are places that exhibit locally high tensile stress values. A longitudinally oriented crack, running lengthwise down the surface of the part, would tend to be opened by a tensile hoop stress. Similarly, a circumferentially oriented crack, running across the body, would be opened by an axial tensile stress.

This assembly was transformed from global to cylindrical coordinate system with the hoop stress component shown.

Figure 22
Hoop stress transformed from global coordinate system

The body was discretized into separate regions; the thread, sidewall, and cup regions. The maximum tensile stress location and values through the cross-section of the body were determined and extracted for each of the three regions. This allows for separate sets of inspection criteria to be determined for different parts of the component. Figure 23 breaks down the three regions of the part that were scrutinized.
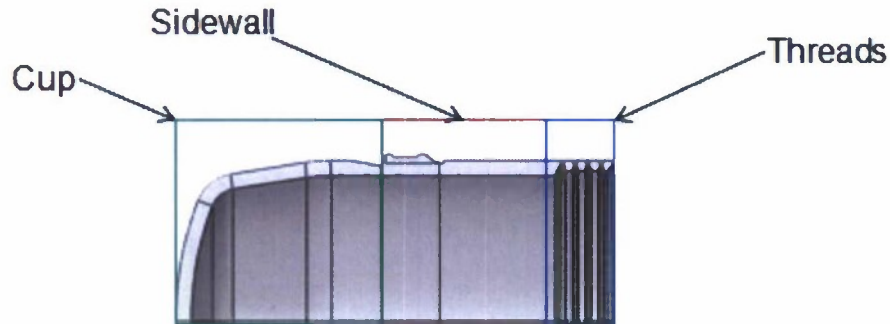
Figure 23
Regions with the body

Within ABAQUS/Viewer, the stress through the sidewall was obtained using the probe results feature, which outputted the S22 stress at various nodes through the sidewall thickness. This extraction was performed at seven different locations in the model at the particular locations of peak stress in hoop and axial. Figure 24 shows an example of the stress state probe at a hotspot below the threaded joint. Several other significant hotspots were probed along the inside of the body, indicated in red on figure 25. Table 2 shows an example of the stress distribution generated from the ABAQUS output.

Figure 24
Location of extracted stress distribution

Figure 25
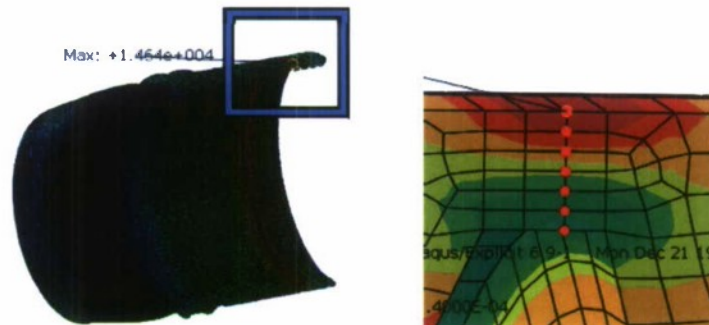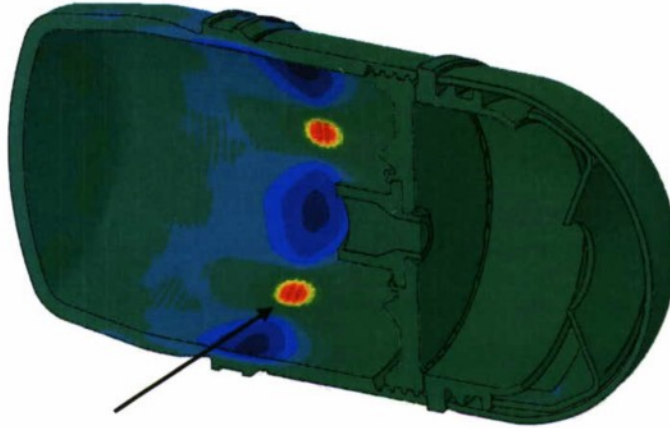Tensile hotspots

Table 2
Example stress distribution

Sidewall	Location (radius, in.)	Hoop stress, tensile (psi)
Outside	0.782	14627.70
	0.77875	12962.90
	0.7755	9593.01
	0.77225	6204.45
	0.769	2670.46
	0.76575	-797.09
Inside	0.7625	-2414.17

These stress gradients were inputted into the NASGRO software cracked models in tabular form. Since the models only assume simple cylindrical shape, only thickness and outer diameter are provided to the code. As a starting point, an initial flaw size of 0.01 in. and a 0.1 a/c ratio (ratio of crack depth to length) are used. NASGRO applies these values to the critical flaw size equation which is

$$a_{cr} = \frac{1}{\pi}\left[K_{max} \Big/ \sum_n S_n F_n \right]^2$$

Where K_{max} is the fracture strength of the material, S_n is based on the stress state, and F_n are coefficients predetermined from FEA studies by NASGRO.

NASGRO

NASGRO uses an iterative approach in solving for a critical crack size and so the solution is dependent on an initial critical flaw size, which is often guessed. Numerical approximation is performed using Newton's method and complicated load cases can yield multiple solutions or be numerically unstable. Care must be taken to estimate an initial trial size that is as realistic and accurate as possible or erroneous results could occur. It is prudent to rerun an analysis with varying initial flaw sizes to verify the results.

In each of the calculations, NASGRO either reported a crack size that was outside the geometric bounds of the problem (larger than the scale of the part) or did not converge after 100 iterations (table 3). When this occurred, the initial flaw size was set at the thickness of the part and re-run. If the code still did not find crick propagation at this trial size, it can be safely inferred that for the given geometry, material, and stress state, the critical flaw size is significantly out of the geometric bounds of the model. From an engineering and manufacturing viewpoint, a large critical flaw size is favorable; if it is approximated that a small critical flaw size pertains to one or more of the parts in the analysis, a costly and time consuming regiment of inspection must be developed for the part in question.

Table 3
Flaw sizes at various locations in the model

Part (stress component)	Location	Calculated flaw size (in.)
Body (hoop)	Sidewall	Out of geometric bounds
Body (hoop)	Thread region	Out of geometric bounds
Body (hoop)	Cup region	Out of geometric bounds
Body (hoop)	Sidewall	0.121
Ogive (axial)	Sidewall	0.293
Fuze body (axial)	Sidewall	0.0165

Since the M433 is a low velocity projectile and uses a reduced amount of propellant for launch, the pressure and inertia loading is smaller compared to higher velocity projectiles in the arsenal. The critical flaw size calculations here indicate that these parts are not overly susceptible to failure by small scale manufacturing flaws as, for example, high velocity tank ammunition and artillery ammunition can tend to be.

Nevertheless, no matter what the load environment a projectile is subject to during launch and travel to the target, it is common practice to use a maximum inspection size of one-fourth of the part thickness in the absence of a critical flaw size analysis that indicates a size smaller. The one quarter rule is a precaution that ensures some factor of safety and acknowledges that most components in an ammunition system are under either a bending or buckling or strain mode, in which tension and compression straddle a neutral axis. It is prudent to not allow and localized plastic deformation or cracks to occupy space anywhere close to the neutral axis to prevent instability.

Oscillatory loading during gun launch and flight can progressively damage material or grow flaws that penetrate significantly into the part thickness. With this in mind, the final inspection criteria reported for the parts are displayed in table 4.

Table 4
Inspection criteria determined from the analysis

| Part	Location	Depth (in.)	Length (in.)
Body	Sidewall	0.014	0.028
Body	Thread region	0.0048	0.0096
Body	Cup region	0.0123	0.0246
Ogive	Whole part	0.007	0.014
Fuze body	Whole part	0.0165	0.0330

CONCLUSIONS

The modeling effort detailed in this report used linear elastic material definitions and linear elastic fracture mechanics to estimate a critical flaw size for the M433 grenade body. The modeling assumed a constant fracture toughness of 35 ksi/in. for steel that yielded relatively large critical crack size values. Though fracture does not appear to be an issue from the results of this analysis, the maximum inspection criteria of one-fourth the total wall thickness is still applicable for the M433. Future work should include further study and validation of the manufacturing process for the M433 body to better understand the formation of defects and ensure acceptable part quality.

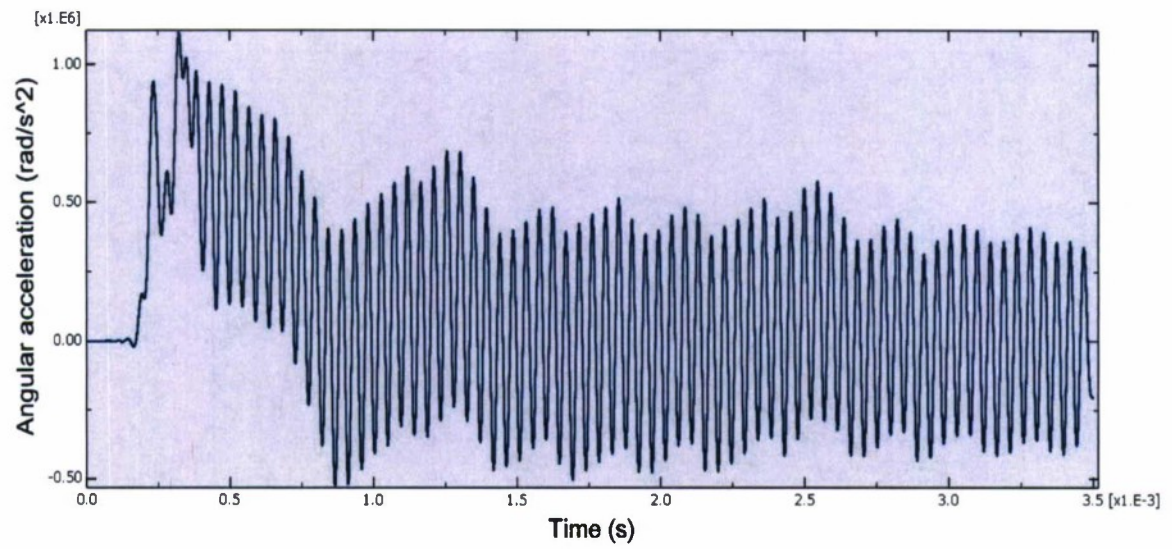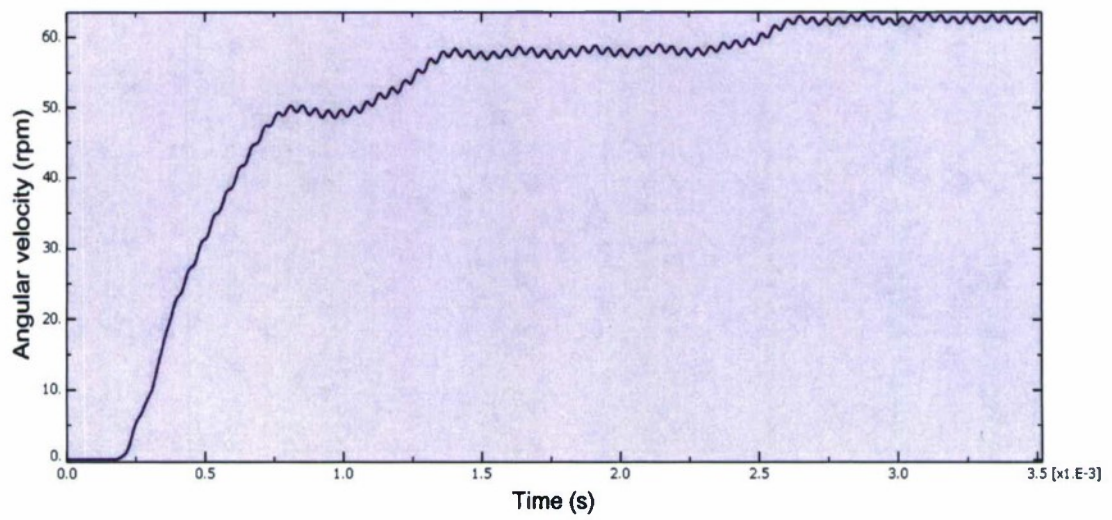APPENDIX
EXPLICIT ANALYSIS DATA PLOTS
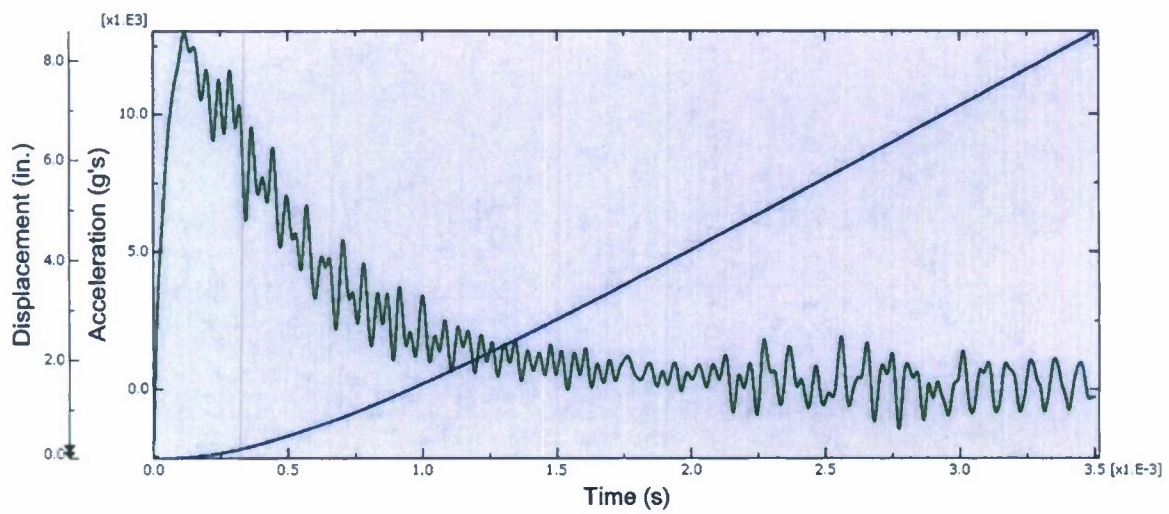
Axial acceleration and displacement at base
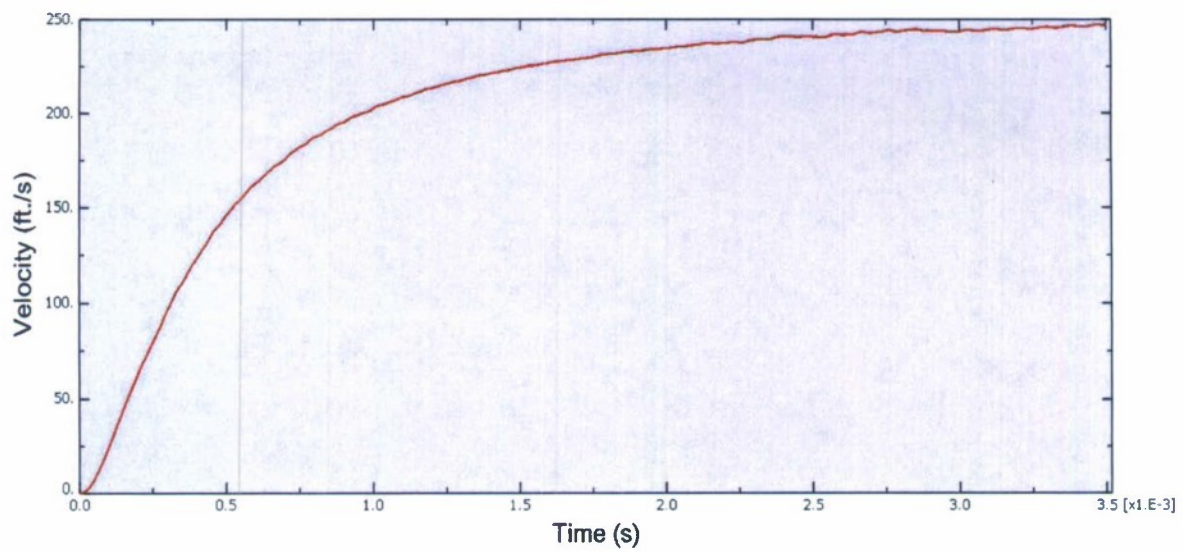
Axial velocity

Angular acceleration at base

Angular acceleration at base

20

BIBLIOGRAPHY

1. Anderson, T. L., <u>Fracture Mechanics, Fundamentals and Applications</u>, CRC Press, Inc., Boca Raton, FL, 2nd edition, pp. 627-636, 1995.

2. Roylance, David, "Introduction to Fracture Mechanics," Massachusetts Institute of Technology, Cambridge, MA, 2001. http://web.mit.edu/course/3/3.11wwmodules/frac.pdf

3. Payne, N.; Jablonksi, J.; and Cordes, J., "Simulia Customer Conference 2010 Proceedings: Determination of Critical Flaw Size in Gun Launched 40mm Grenade," Conference proceedings, Dassault Systems, Providence, RI, 2010.

DISTRIBUTION LIST

U.S. Army ARDEC
ATTN: RDAR-EIK
        RDAR-GC
        RDAR-MEF-E, J. Jablonski
                    J. Cordes
                    N. Payne (3)
                    P. Carlucci
                    J. John
Picatinny Arsenal, NJ 07806-5000

Defense Technical Information Center (DTIC)
ATTN: Accessions Division
8725 John J. Kingman Road, Ste 0944
Fort Belvoir, VA 22060-6218

Commander
Soldier and Biological/Chemical Command
ATTN: AMSSB-CII, Library
Aberdeen Proving Ground, MD 21010-5423

Director
U.S. Army Research Laboratory
ATTN: AMSRL-CI-LP, Technical Library
Bldg. 4600
Aberdeen Proving Ground, MD 21005-5066

Chief
Benet Weapons Laboratory, WSEC
U.S. Army Research, Development and Engineering Command
Armament Research, Development and Engineering Center
ATTN: RDAR-WSB
Watervliet, NY 12189-5000

Director
U.S. Army TRADOC Analysis Center-WSMR
ATTN: ATRC-WSS-R
White Sands Missile Range, NM 88002

Chemical Propulsion Information Agency
ATTN: Accessions
10630 Little Patuxent Parkway, Suite 202
Columbia, MD 21044-3204

GIDEP Operations Center
P.O. Box 8000
Corona, CA 91718-8000